Anchorage and residual bond characteristics of 7-wire strand
Orr *et al*

Highlights

- 31 specimens with 7-wire strand are subject to pull out tests;
- The effects of inadequate cover and reinforcement detailing are investigated;
- Specimens with negative cover can retain significant pull out capacity;
- Confinement from transverse reinforcement and cover must be considered together;
- A capacity assessment method is proposed.

Abstract

The periodic assessment of our existing concrete infrastructure is a crucial part of maintaining appropriate levels of public safety over long periods of time. It is important that realistic predictions of the capacity of existing structures can be made in order to avoid unnecessary and expensive intervention work. Assessment is currently undertaken using codified models that are generally readily applied to infrastructure with simple geometric and reinforcement details that conform to design methods for new structures.

This approach presents two significant challenges for prestressed structures: 1) design and construction practice has changed significantly in the past 50 years, and modern codified approaches can be incompatible with historic structures; and 2) deterioration of exposed soffits can lead to reduced cover to internal prestressing strand. Unless appropriate reductions are used in assessment of a structure with such problems, unnecessary load restrictions, or major strengthening or reconstruction work may be required, despite having carried a full service load since its construction.

There are currently no widely accepted methods for the prediction of peak and residual capacities in prestressed concrete beams with inadequately detailed 7-wire strand. This paper presents a completely new prediction methodology, validated against new experimental results from 31 novel semi-beam tests. The proposed models for peak load, residual load, and bond stress-slip modelling provide reliable, accurate, and conservative results. Their results demonstrate feasible and appropriate capacity reduction factors for use in the assessment of existing concrete infrastructure.

Notation

$ø$	Nominal strand diameter (mm)
d	Effective depth to flexural reinforcement (mm)
c	Cover to strand (mm)
b	Breadth (mm)
L	Length (mm)
δ_1	Modification factor accounting for reduced cover
δ_2	Modification factor accounting for confinement from cover and/or transverse reinforcement
δ_3	Modification factor accounting for confinement from transverse reinforcement
δ_4	Modification factor accounting for confinement from cover
F	Force (N)
σ_{pd}	Strand Stress (MPa)
A_{ps}	Cross sectional area of strand (mm^2)
l_{bpd}	Total anchorage length for anchoring a tendon with stress σ_{pd} (mm)
l_{pt2}	120% of the basic transmission length (mm)
σ_{pd}	Prestress after all losses (MPa)
σ_{pm0}	Tendon stress just after release (MPa)
f_{bpd}	Bond strength of the concrete at the test date (MPa)
f_{bpt}	Bond stress at transfer (MPa)
$f_{ctd(t)}$	Axial tensile strength of the concrete at release (MPa)
f_{ctd}	Axial tensile strength of the concrete (MPa)
$f_{ctm(te)}$	Mean axial tensile strength at the test date (MPa)
$f_{ctm(tr)}$	Mean axial tensile strength measured at transfer
$\tau_{b,max}$	Maximum value of bond stress (MPa)
s	Slip (relative displacement of strand and concrete) (mm)
L_b	Bonded length (mm)
R_m	Strand tensile strength (MPa)

1 Introduction

The periodic assessment of existing infrastructure is crucial to maintain appropriate levels of safety over long periods of time. Changes in loading, material properties, design, detailing, and construction practices mean that some infrastructure, when assessed today, is deemed to be structurally inadequate. Assessment methods that can properly and accurately predict the behaviour of such structures are therefore crucially important to avoid unnecessary and expensive reconstruction works.

Road infrastructure provides a crucial economic pathway, and trunk route road closures have significant economic impacts. Minimising closures to bridges and other infrastructure for repair can therefore provide economic benefits. In the USA, 67,000 (11%) of bridges have been deemed as structurally deficient with load restrictions or closures, and the ASCE estimates $76 billion is required for their repair or replacement [1]. In the UK road infrastructure investment of £15 billion is already planned for the period to 2021 [2]. Such levels of repair and refurbishment are significant, and must be supported by the provision of appropriate assessment methodologies.

1.1 Half joint bridges

Half joints (Figure 1) have historically been used to simplify the design and construction of bridges. However, due to inspection, construction, and maintenance problems with such designs BD 57 [3] cl.2.2 now notes that half joints should not be used for new bridges unless there is absolutely no alternative. The structural assessment of structures containing half-joints at the serviceability and ultimate limit states in the UK is undertaken using strut and tie models in accordance with BD 44 [4] and BA 39 [5]. Such approaches are readily applicable to cases with simple geometric and reinforcement detailing and when the reinforcement is appropriately anchored.

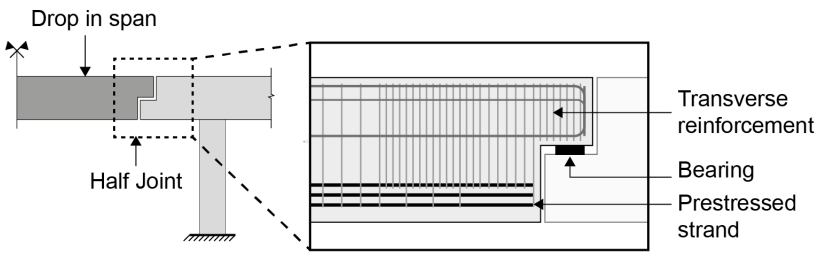

Figure 1: Half joint bridges

If reinforcement in existing structures does not provide theoretically sufficient anchorage to be fully utilised in a strut and tie model, reduction factors are applied by the assessing engineer. Common issues where this may arise include 1) loss of cover due to environmental deterioration; 2) inadequate cover from design detailing; and 3) transverse reinforcement that does not enclose longitudinal reinforcement. A modern assessment of a structure with such problems, which may have carried the full service load since its construction, could lead to load restrictions, strengthening or reconstruction work, if realistic and appropriate assessment methods, including consideration of reliability and reduction factors, are not known and used.

Some half joint bridges assessed using BD 44 [4] and BA 39 [5] have recently been rated as provisionally substandard. Although such bridges are now being traffic managed using BD 79 [6], they had previously been carrying unrestricted traffic loading since their construction in the 1970s.

This paper investigates the effect of loss of cover on bond, peak load, and residual behaviour for specimens with 7-wire strand as flexural reinforcement. A series of semi-beam pull out tests were undertaken utilising both unstressed and pretensioned strand to develop new guidance on appropriate reduction factors for the assessment of half-joint bridges and, in general, prestressed concrete elements containing theoretically inadequate 7-wire strand detailing.

2 Bond and anchorage

2.1 Bond tests

Tests are required to determine the bond characteristics of concrete reinforcement in order to effectively predict required transmission (transfer) and anchorage (development) lengths. Simple cube pull out tests are commonly used (see for example RILEM [7] and ASTM [8] methods) and considerable data for these exists [9-12]. Such tests, however, provide very localised data over small bonded lengths. BS 4449 [13] overcomes this limitation through the use of a half-beam test setup, similar to the 'beam end test' of ASTM A944 [14].

A simplification of the half-beam test method was proposed by Perera *et al* [15] in which one half of the specimen is tested, whilst retaining the correct state of stress in the end zone. This approach has numerous advantages, including a simpler test set up, and the ability to keep the bar straight rather than deforming it under loading. This method was adopted in this paper for testing unstressed specimens (Figure 4).

2.2 Strand bond

2.2.1 Unstressed strand

The majority of previous studies of bond of prestressing strand, has been on unstressed samples. Unstressed 7-wire strand achieves bond with the surrounding concrete through adhesion and mechanical interlock. Once slip occurs, adhesion is no longer present and bond will therefore rely only on the mechanical interlock provided by the helical shape of the strand. Unlike for plain and deformed passive reinforcement [16], there is no well-established bond stress-slip model for prestressing strand, yet such a model is crucial for the realistic assessment of existing structures.

To determine the bond-slip performance of steel wire strand, Moustafa [17] developed a pull out test in which multiple strands are pulled from a large concrete block, while the Post-Tensioning Institute (PTI) Bond Test uses a single strand pulled from a cement mortar cylinder. The North American Strand Producers (NASP) Bond Test was derived from the PTI method and subsequently adopted by the USA Transport Research Board [18]. The strand is pulled from the cylinder at 24 hours, with the free-end slip of the strand measured. A revised version of the NASP bond test is the Standard Test for Strand Bond (STSB), adopted by the ASTM [19]. Pull out forces and slips are measured for the strand cast into a mortar cylinder. The NASP test provides only a proxy result since the strand is tested in a cylinder of mortar, with the pull out value then being correlated to codified requirements for transmission lengths for strand in concrete.

Logan [20] performed 216 pull out tests on 13mm diameter strands from six different manufacturers using the method proposed by Moustafa [17], and showed considerable variation in performance between manufacturers. When compared to flexural beam tests it was however found that the pull out was a useful proxy for comparing behaviour. The variation between manufacturers is also reported by Ramirez and Russell [18] during round robin testing using the NASP test. This suggests that characterising as far as possible properties of the actual strand used in any beam to be assessed is important.

Rose and Russell [21] reported an increase in bond strength for strand with a uniform surface coating of rust (achieved over a period of three days exposure in high humidity, wet spray environment) prior to casting. Their work assessed the effects of strand with minor corrosion being used in new construction, and as such may not be not representative of the effect of rusting a steel strand in-situ (which implies that the environmental conditions within the concrete have changed, for example through loss

of alkalinity of the concrete or loss of concrete cover), which would seriously compromise the strand to concrete bond.

2.2.2 Stressed strand

In addition to adhesion and mechanical bond, stressed strand obtains further anchorage from the 'Hoyer effect' [22]. The Hoyer effect occurs after the stress in the strand is released into the concrete. Elastic expansion, dilation, and helical strain in the strand result in radial forces in the concrete. These radial forces enhance friction and provide a wedge effect.

The length over which prestress force is transferred into the concrete section may be determined by measuring slip at the end of a concrete member and strain on the concrete face parallel to the strand after release of the prestress, while anchorage lengths are typically assessed using pull out tests on unstressed strands as described above.

The challenge of achieving a robust test method for prestressed strand is discussed by Marti-Vargas *et al* [23]. Building on work by Cousins *et al* [24], Marti-Vargas *et al* [23] proposed a test method that uses a concentrically positioned pretensioned bar pulled out of a concrete prism, referred to as the 'ECADA' test. Testing a range of prism lengths allows the anchorage and transmission lengths to be estimated and provides load-slip responses for different embedment lengths.

Higher strength concretes (up to 80MPa) typically allow shorter anchorage lengths [24]. Barnes and Burns [25] found an inversely proportional relationship between the concrete strength and transmission length, although significant scatter was also seen in the test data.

2.2.3 Effect of loss of cover on strand bond

BS EN 1992-1-1 [26] specifies that the minimum cover required to maintain bond to 7-wire strand is *1.5ø*, where *ø* is the strand diameter (greater cover may be required for other reasons). Force transfer between the tendon and the concrete is modelled by Tepfers [27] using radially directed compressive stresses equilibrated by circumferential tensile stresses. The confining effect of the concrete is determined by the maximum tensile stress that can be carried before cracking of the concrete. Splitting failure can occur when cover distances are low [28]. Various models in the literature use this approach to determine the effect of concrete cover on transmission and anchorage lengths [29].

There have been very few tests on specimens with stressed 7-wire strand where cover distance was a test variable. Deatherage and Burdette [30] tested full scale bridge girders with cover of between *2.5ø* and *3ø* and found no difference in anchorage lengths for 15mm strand, an unsurprising result given the BS EN 1992-1-1 [26] limit above. Den Uijl [31] tested smaller specimens with cover distances between *1.36ø* and *3.0ø* to determine minimum cover requirements to prevent splitting failures. A reduction in transmission length as cover increases was found, proposed to be due to the non-linear response of the concrete to the wedging effect at tendon release.

Despite a large amount of testing of cube and half-beam specimens to determine bond characteristics of specimens with adequate cover distances (well designed specimens) no data was found in the literature for such semi-beam tests where the test bar has low or negative cover distance (i.e the reinforcement is partially exposed), a key focus of this paper.

2.2.4 Effect of corrosion on strand bond

Rogers *et al* [32] performed destructive tests on 19 decommissioned bridge beams dating from 1969, all of which had suffered corroded pre-tensioned reinforcement due to a high-chloride environment. The beams contained both pretensioned and post-tensioned reinforcement, had a design concrete strength of 38MPa, and mild steel transverse reinforcement. Twelve pre-tensioned strands of 12.7mm diameter were used in each beam, and these strands were unenclosed by the transverse reinforcement. Longitudinal cracking in the soffit of the beams was noted during inspections, subsequently found to be a result of chloride induced corrosion propagating from the corner strand into the specimen until delamination of the cover zone occurred.

The 19 beams were tested in three point bending. A combination of shear and flexural failures was recorded. The corroded beams showed between 10% and 32% loss in capacity when compared to beams in a 'good' condition. The magnitude of the capacity reduction was approximately in line with the loss of pre-tensioned strand due to corrosion. The authors' results suggest that the use of non-destructive methods to determine corrosion in strand can be used as an indicator of the actual capacity of a beam under assessment.

2.3 Summary

A broadly accepted model for the pull out characteristics of prestressing strand is not currently available as it is for plain and deformed bars. It is noted in much of the literature that cover distances are important for determining splitting or pull out failures, especially when the presence of transverse reinforcement can confine concrete around the strand. However no data is available for the pull out testing of beams with strand that has low or negative cover distances. This is important since corroded or spalled

structures may have such low (or negative) cover and their residual capacity needs to be able to be quantified.

3 Testing

To determine the pull out behaviour of 15.2mm diameter 7-wire strand and provide new guidance on appropriate reduction factors for assessment, a series of semi-beam tests were undertaken to determine for the first time the effect of loss of cover on bond, peak load, and residual load in specimens with both unstressed and pretensioned strand.

3.1 Test design

A total of 31 semi-beam specimens were tested, 19 with unstressed strand and 12 with stressed strand. Both stressed and unstressed specimens were tested in order to identify any specific pull out behaviour arising from prestressing of the strand. All specimens were designed with an effective depth to the strand of 300mm and breadth of 200mm. All strand was 15.2mm in diameter (ø). The test variables were: bonded length (300mm (≈20ø), 600mm (≈40ø), or 900mm (≈60ø)), cover distance to the strand (37mm, 0mm, or -8mm), and transverse reinforcement design (Plain ('P'), Enclosed ('E'), or Unenclosed ('U'), as shown in Figure 2). The specimens are summarised in Table 1.

Specimens with negative cover (-8mm) have half the diameter of the strand outside of the concrete section. For specimens with -8mm cover *and* enclosed transverse reinforcement ('E'), the transverse reinforcement necessarily also sits outside the concrete section. See also Figure 14.

The prismatic test specimens have a support condition beneath the strand, whereas this is more remote in a real half-beam joint. The pragmatic test set up was chosen to reflect reality as far as possible, but it is important to realise this potential limitation.

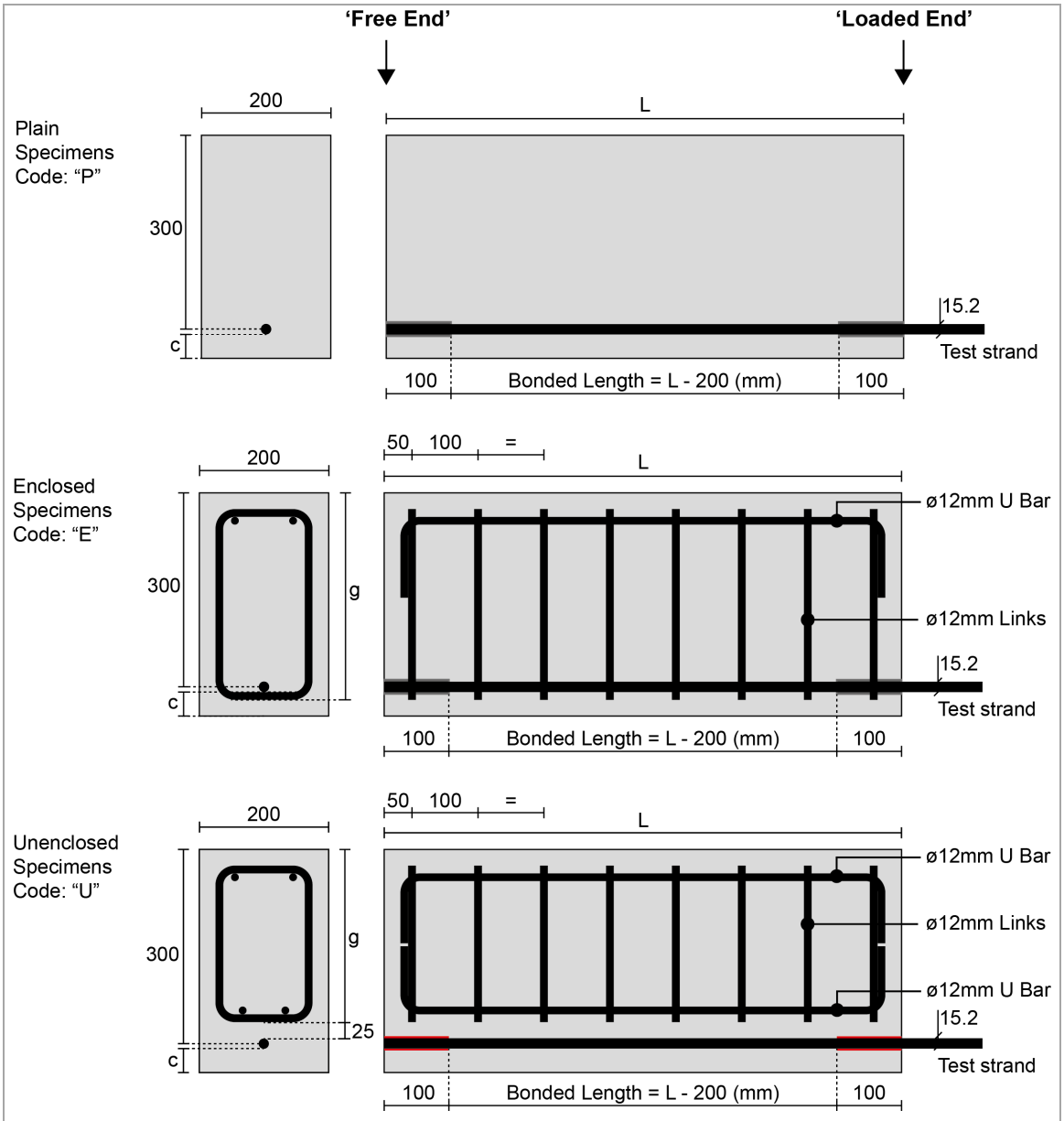

193

194 **Figure 2: Specimen dimensions**

195 **Table 1: Test specimen details**

Specimen Code[a]	Initial prestress (% R_m)	Transverse reinforcement type[b]	Dimension g (mm)[c]	Length, L (mm)[d]	Bonded length (mm)[e]	Cover, c (mm)[f]
0/P/300/37	0	P	0	500	300	37
0/P/300/0	0	P	0	500	300	0
0/P/600/37	0	P	0	800	600	37
0/P/600/0	0	P	0	800	600	0
0/E/300/37	0	E	320	500	300	37
0/E/300/0	0	E	320	500	300	0
0/E/300/-8	0	E	320	500	300	-8
0/E/600/37	0	E	320	800	600	37

Specimen Code[a]	Initial prestress (% R_m)	Transverse reinforcement type[b]	Dimension g (mm)[c]	Length, L (mm)[d]	Bonded length (mm)[e]	Cover, c (mm)[f]
0/E/600/0	0	E	320	800	600	0
0/E/600/-8	0	E	320	800	600	-8
0/E/900/37	0	E	320	1100	900	37
0/E/900/0	0	E	320	1100	900	0
0/E/900/-8	0	E	320	1100	900	-8
0/U/600/37	0	U	267	800	600	37
0/U/600/0	0	U	267	800	600	0
0/U/600/-8	0	U	267	800	600	-8
0/U/900/37	0	U	267	1100	900	37
0/U/900/0	0	U	267	1100	900	0
0/U/900/-8	0	U	267	1100	900	-8
55/E/600/37	55	E	320	800	600	37
55/E/600/0	55	E	320	800	600	0
55/E/600/-8	55	E	320	800	600	-8
69/E/900/37	69	E	320	1100	900	37
69/E/900/0	69	E	320	1100	900	0
69/E/900/-8	69	E	320	1100	900	-8
55/U/600/37	55	U	267	800	600	37
55/U/600/0	55	U	267	800	600	0
55/U/600/-8	55	U	267	800	600	-8
69/U/900/37	69	U	267	1100	900	37
69/U/900/0	69	U	267	1100	900	0
69/U/900/-8	69	U	267	1100	900	-8

Notes: [a] Specimen Code:Initial Prestress % [0 (unstressed), 55%, or 69%] / Transverse Reinforcement Type [P, E, U, Figure 5] / Bonded Length [300, 600, or 900mm] / Cover [37, 0, or -8mm], [b,c,d,e,f] See Figure 5.

3.1.1 Design parameters

An average concrete cube compressive design strength of 50MPa for all specimens was chosen, to replicate typical concrete strengths found in historic examples of prestressed concrete beams provided by Highways England. A concrete mix was designed to achieve a compressive strength of 50MPa at the test date (14 days after casting) and is given in Table 2. Six 100mm cubes and 100mm cylinders were cast alongside each test specimen in accordance with BS EN 12390-2 [33] for compressive strength testing [34] and tensile splitting testing [35]. All specimens were demoulded 24 hours after casting.

Bridon 7-wire 15.2mm diameter 1670 Grade strand was used in all specimens, Table 3. A tension test was undertaken on a sample of the 15.2mm diameter strand, as shown in Figure 3, where stresses are calculated using a cross sectional area of 139mm^2 (Table 3).

Bonded lengths of 300, 600, and 900mm were chosen based on prediction calculations following BS EN 1992-1-1 [26] such that all specimens would fail in pull out (rather than strand yield) whilst also giving a range of bonded areas to consider in the analysis.

Where present, all other reinforcement in the test specimens was 12mm diameter deformed bar grade B500C [36]. Cover to the transverse reinforcement was 25mm. None of the specimens with transverse reinforcement failed in shear.

Table 2: Mix design per m^3

CEM I 42.5N Cement (kg)	**Tap water (kg)**	**Coarse aggregate (12-14mm)**	**Fine aggregate (<5mm)**
620	210	865	710

Table 3: 1670 Grade Strand, manufacturer's data [37] following prEN 10138 [38]

Type	Nominal diameter (mm)	Nominal values only				Specified characteristic values		Typical values
		Tensile strength (R_m) N/mm^2	Steel area (mm^2)	Mass (kg/m)	Mass (m/1000kg)	Breaking load (F_m) kN	0.1% Proof load ($F_{p0.1}$) kN	Load at 1% elongation (Ft 1.0) kN
Standard	**15.2**	**1670**	**139.0**	**1.090**	**917**	**232.0**	**204.0**	**204**

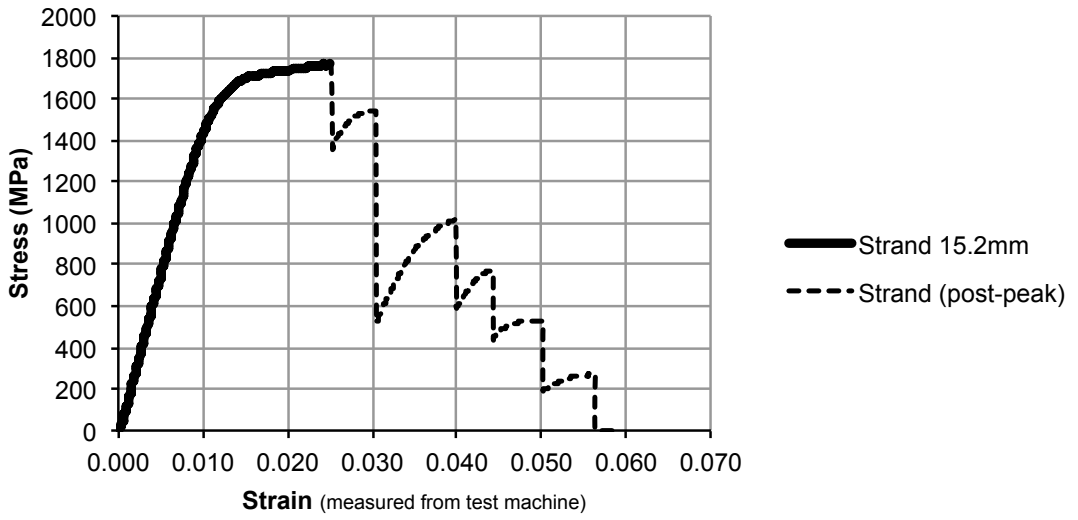

Figure 3: Load-displacement results for 15.2mm strand as tested

3.1.2 Stressed strand specimens

Twelve specimens were tested with pre-tensioned strand. The specimens had bonded lengths of 600mm or 900mm (Table 1). Strand stresses were chosen based on information provided by Highways England for historic stressed strand specimens. Specimens with 600mm bonded length were pretensioned to an initial stress of 916MPa ($0.55R_m$) and specimens with 900mm bonded length were pretensioned to 1145MPa ($0.69R_m$).

3.2 Test method

3.2.1 Unstressed specimens

All specimens were tested 14 days after casting in the frame shown in Figure 4. Load was applied to each strand by a 2000kN test machine under stroke control at 2mm/min. Slip of the strand was measured using linear variable displacement transducers at both the test end and the free end of the specimen (LVDT1 and LVDT2).

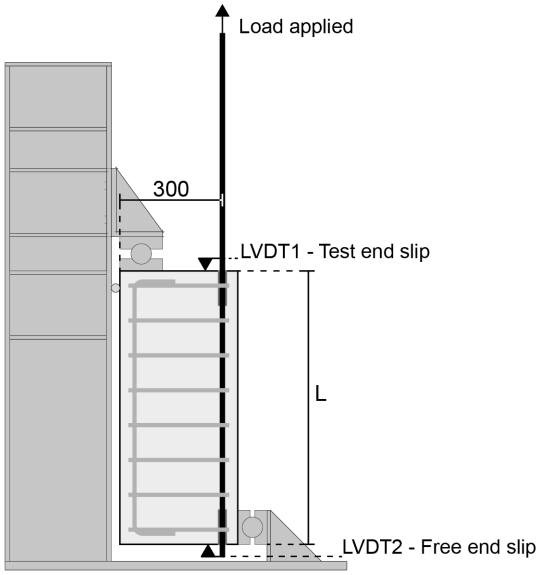

Figure 4: Unstressed specimen test method

3.2.2 Stressed specimens

In a prestressed beam a transmission length is required at both ends of the strand. When calculated using BS EN 1992-1-1 [26] the transmission length is linearly related to the tendon stress after release. Therefore a high tendon stress requires a longer transmission length. To achieve the semi-beam test method with prestressed strand, it was necessary to maintain the strand tension at the test end of the specimen (Figure 2) throughout the casting and curing process. This was achieved by stressing, casting and testing these specimens in pairs in a bespoke frame (see Figure 5).

Hydraulic jacks were used to apply and maintain the pretension during casting and curing. After three days the strand stress was released at the free end but was maintained at the test end by allowing the specimen to react against the test frame cross beam (Figure 5). After curing, the jacks at the test end of the frame were used to apply the test load to the stressed strand (Figure 6). One load cell per strand was used to monitor the strand force throughout the prestressing, curing, and testing phases.

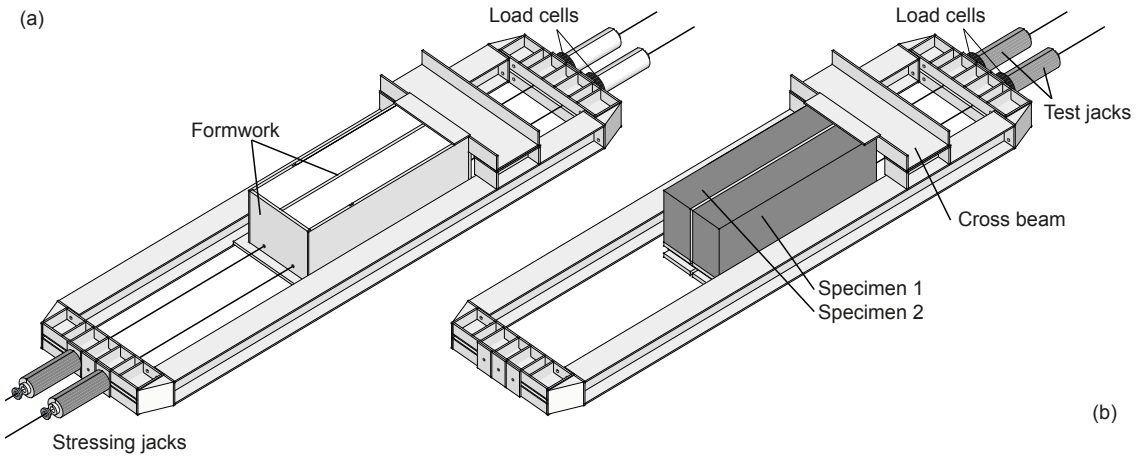

Figure 5: Stressing and casting arrangement (a); Test arrangement (b)

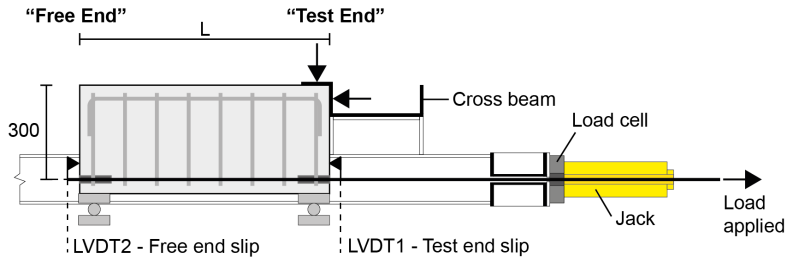

Figure 6: Test method, stressed specimens

3.3 Results

3.3.1 Concrete strength

The average concrete compressive cube strength at the test date was 54.2MPa (with a standard deviation of, σ = 4.8MPa from 81 tests). The average concrete split cylinder tensile strength of all specimens at their test date was 3.52MPa (σ = 0.68MPa from 48 cylinders). For specimens with stressed strand, the average split cylinder tensile strength at strand detensioning (3 days after casting) was 3.41MPa (σ = 0.68MPa from 11 cylinders).

3.3.2 Prestress losses

For the prestressed specimens, load cells were used to monitor the strand stress throughout their casting, curing and strand detensioning. The load-time results all

followed the same pattern, as summarised in Figure 7. Results for each specimen are given in Table 4. The strand stress prior to testing after all losses ($\sigma_{pm\infty}$) is given by Point 4.

It is apparent in Table 4 that losses in Specimens 69/U/900/0 and 69/U/900/-8 are so large as to imply that slip in the prestress zone was sufficient to break the bond between the strand and the concrete. As shown in Figure 5, the specimens were cast in pairs. Premature detensioning occurred in the specimen cast alongside 69/E/900/-8, which caused a small increase in the Point 2 value of prestress recorded for 69/E/900/-8 (see Table 4). The increase was small enough to not be a concern. The specimen that suffered premature detensioning was not tested.

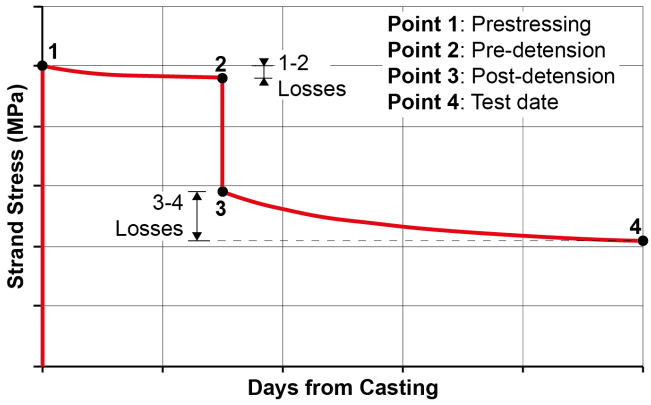

Figure 7: Typical prestress loss over time indicating Points 1 – 4 in Figure 7

Table 4: Summary of prestress losses

Code[1]	Cover	Target Prestress	Point 1	Point 2	1-2 Loss (%)	Point 3	Point 4	3 - 4 Loss (%)	Total losses (1-4) (%)
55/E/600/37	37	916MPa	1016MPa	962MPa	5%	626MPa	551MPa	12%	46%
55/E/600/0	0	916MPa	1009MPa	966MPa	4%	575MPa	419MPa	27%	58%
55/E/600/-8	-8	916MPa	993MPa	996MPa	0%	529MPa	428MPa	19%	57%
69/E/900/37	37	1145MPa	1262MPa	1204MPa	5%	955MPa	926MPa	3%	27%
69/E/900/0	0	1145MPa	1261MPa	1233MPa	2%	870MPa	642MPa	26%	49%
69/E/900/-8	-8	1145MPa	1260MPa	1317MPa	-5%	923MPa	693MPa	25%	45%
55/U/600/37	37	916MPa	1004MPa	990MPa	1%	902MPa	871MPa	3%	13%
55/U/600/0	0	916MPa	1000MPa	989MPa	1%	709MPa	464MPa	35%	54%
55/U/600/-8	-8	916MPa	998MPa	1002MPa	0%	631MPa	439MPa	30%	56%
69/U/900/37	37	1145MPa	1256MPa	1241MPa	1%	1144MPa	1091MPa	5%	13%

69/U/900/0	0	1145MPa	1258MPa	1251MPa	1%	478MPa	296MPa	38%	76%
69/U/900/-8	-8	1145MPa	1296MPa	1271MPa	2%	267MPa	172MPa	36%	87%

3.3.3 Peak load

A summary of the peak load achieved in all tests is given in Figure 8, showing peak load divided by bonded length (N/mm) against cover divided by strand diameter. A reliable trend is seen in all cases. Further details are given in Table 5 and Table 6 below.

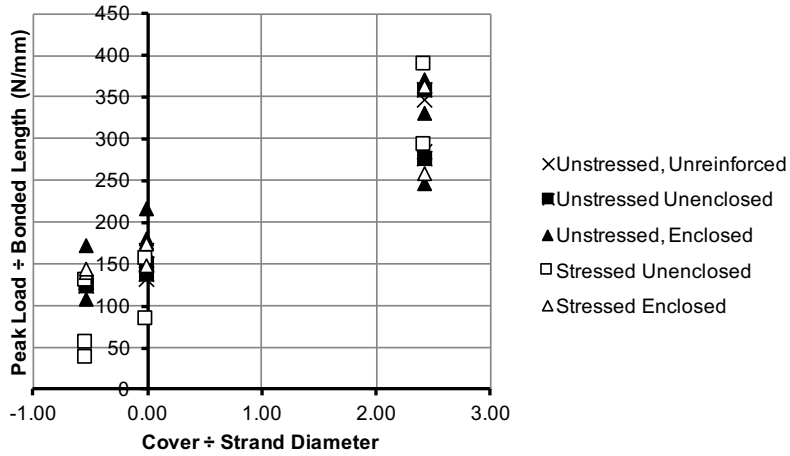

Figure 8: Summary of all peak load results

3.3.3.1 Unstressed specimens

The peak and residual loads for each unstressed test are summarised in Table 5. The applied load versus free end slip is shown in Figure 9 to Figure 11. When represented on the *x*-axis of a graph the slip of the strand is defined as the movement of the strand relative to the specimen concrete face. This is measured with an LVDT secured to the strand with the probe touching the concrete face. Slip at both the *free end* and the *test end* was recorded for the tests (Figure 4).

Table 5: Summary of unstressed specimen test results

Code[1]	Peak Load (kN)	Failure Mode	Residual strength (kN)
0/P/300/37	85	Shear	0
0/P/300/0	50	Pull out	47
0/P/600/37	208	Pull out, Shear	0

Code[1]	Peak Load (kN)	Failure Mode	Residual strength (kN)
0/P/600/0	79	Pull out	70
0/E/300/37	111	Pull out	108
0/E/300/0	65	Pull out	62
0/E/300/-8	52	Pull out	46
0/E/600/37	199	Pull out	0
0/E/600/0	108	Pull out	100
0/E/600/-8	65	Pull out	57
0/E/900/37	223	Pull out	-
0/E/900/0	159	Pull out	158
0/E/900/-8	124	Pull out	120
0/U/600/37	216	Pull out	-
0/U/600/0	83	Pull out	73
0/U/600/-8	77	Pull out	70
0/U/900/37	250	Pull out, block failure	168
0/U/900/0	136	Pull out	130
0/U/900/-8	112	Pull out	74
Notes: [1] See Figure 2 and Table 1.			

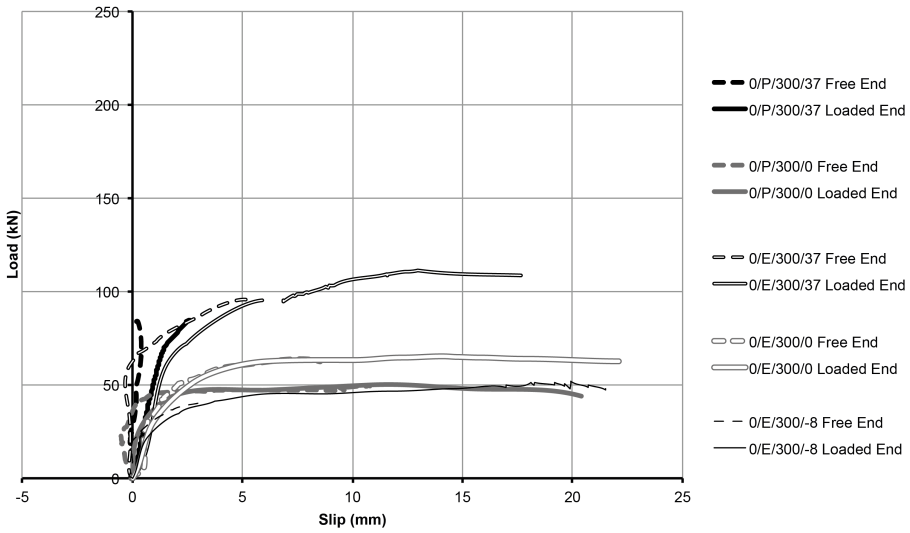

295

296 **Figure 9: Unstressed specimens with 300mm bonded length**

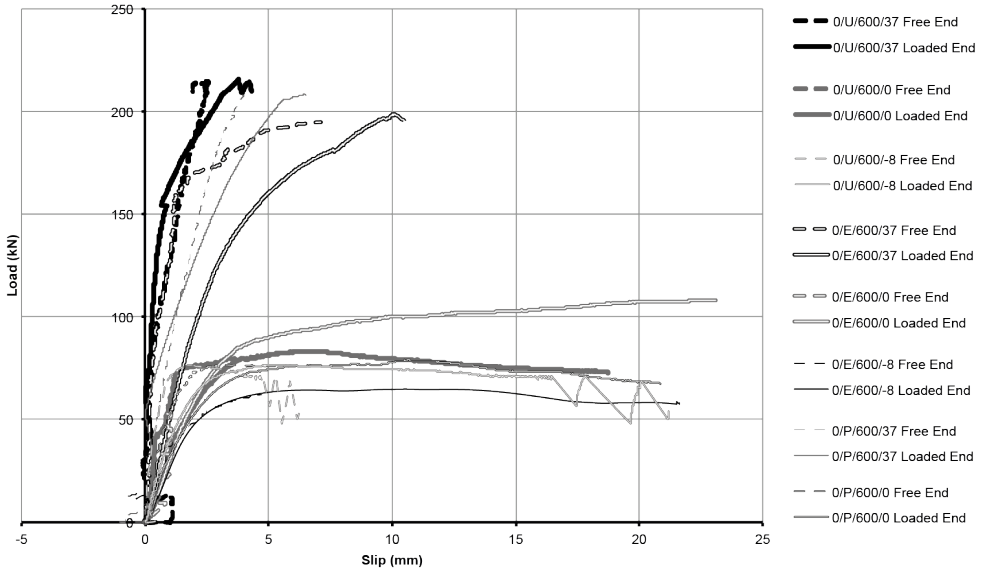

297

298 **Figure 10: Unstressed specimens with 600mm bonded length**

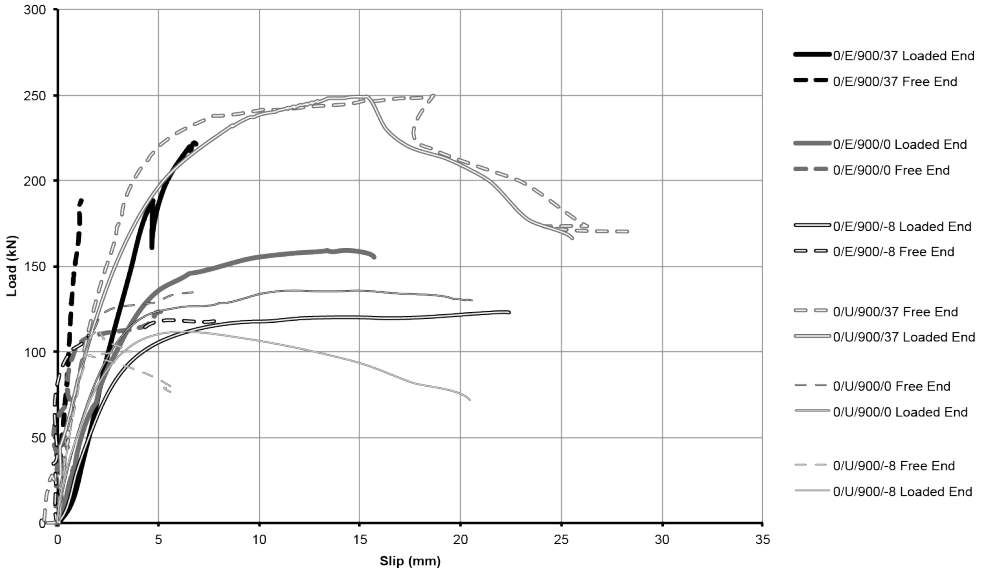

299

300 **Figure 11: Unstressed specimens with 900mm bonded length**

301 *3.3.3.2 Load-slip results – stressed specimens*

302 The peak and residual loads for each stressed test are summarised in Table 6. The

303 applied load versus free end slip is shown in Figure 12 - Figure 13.

304 **Table 6: Summary of stressed specimen test results**

Code[1]	Peak Load (kN)	Failure Mode	Residual strength (kN)
55/E/600/37	217	Pull out	214
55/E/600/0	105	Pull out	100
55/E/600/-8	84	Pull out	64
69/E/900/37	195	Pull out	195
69/E/900/0	131	Pull out	90
69/E/900/-8	129	Pull out	65
55/U/600/37	233	Pull out	233
55/U/600/0	93	Pull out	69
55/U/600/-8	78	Pull out	65
69/U/900/37	264	Strand failure	0
69/U/900/0	77	Pull out	46
69/U/900/-8	34	Pull out	21

Notes: [1] See Figure 2 and Table 1.

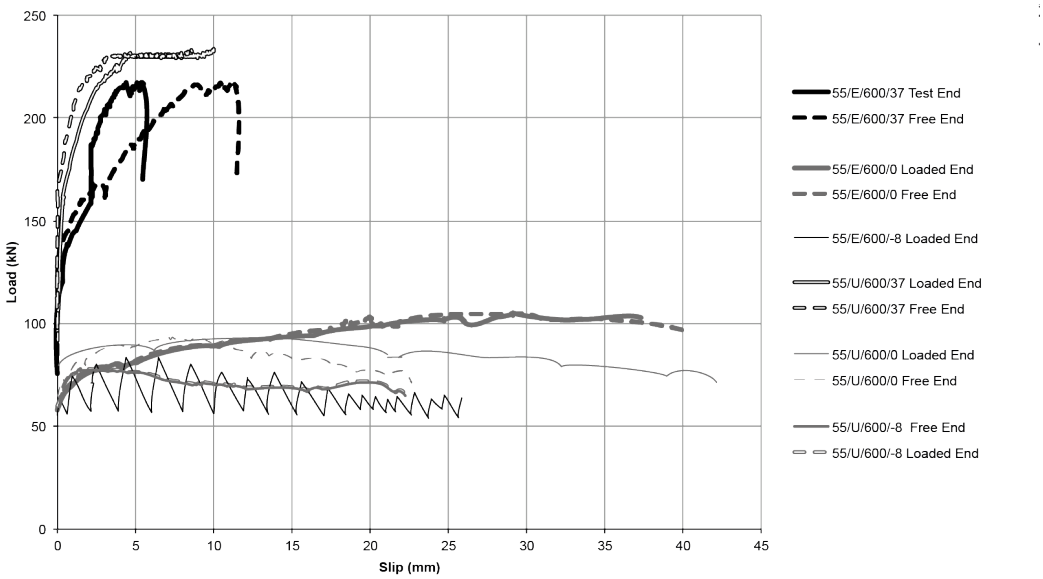

305

306 **Figure 12: Stressed specimens with 600mm bonded length**

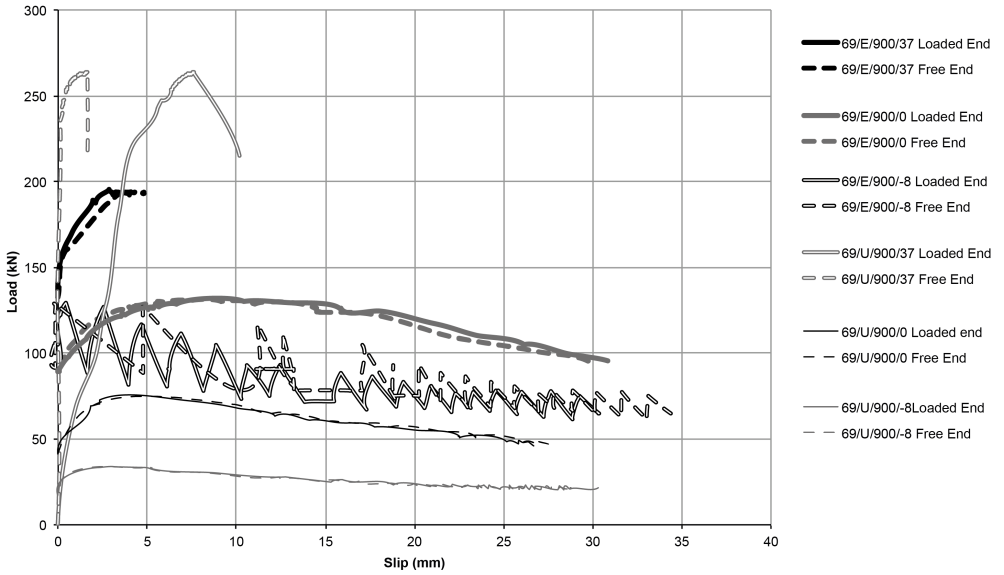

307

308 **Figure 13: Stressed specimens with 900mm bonded length**

309 Specimens 55/E/600/-8 and 69/E/900/-8 both exhibited the same behaviour during
310 post-peak pull out. The 'zig-zag' lines shown in Figure 12 (Specimen 55/E/600/-8) and
311 Figure 13 (Specimen 69/E/900/-8) demonstrate a 'stick-slip' behaviour which was not
312 seen in any other tests. Both specimens have the same transverse reinforcement, and
313 -8mm cover, suggesting that the response may be due to the exposed transverse
314 reinforcement providing additional restraint to the strand during pull out. The maximum
315 peak-peak amplitude of the stick-slip response is 45kN for 69/E/900/-8 and 27kN for
316 55/E/600/-8, the ratio of these two amplitudes is 1.67. This is very similar to the ratio of
317 the number of stirrups crossing the strand in each specimen: nine stirrups enclose
318 69/E/900/-8 and six stirrups enclose 69/E/900/-8 (ratio of 1.5), suggesting that the
319 stick-slip behaviour is indeed related to the localised behaviour provided by the stirrups
320 in these tests.

321 ## 3.4 Summary

322 The tests undertaken have demonstrated that specimens with zero or negative cover
323 can show considerable peak capacity despite their loss of cover. It is seen in the test

results that specimens with transverse reinforcement that does not enclose the strand reached similar peak loads to those for which the transverse reinforcement did enclose the strand. Unenclosed specimens provided capacity in excess of what might be expected of a structure in which there is no obvious tension tie between the strand and the compression zone. Specimens with -8mm cover provided significant levels of peak capacity, but post-peak these specimens displayed a descending load-slip curve and provided no plateau at the peak load.

4 Analysis and Modelling

4.1 Anchorage force

It is proposed that the anchorage capacity of pretensioned beams with inadequate cover can be analysed following the method of BS EN 1992-1-1 [26] Figure 8.17 and applying modification factors that allow the consideration of 1) bonded perimeter (δ_1) and 2) confinement from cover and/or transverse reinforcement (δ_2).

It is proposed that the anchorage force capacity (kN) of members with inadequate cover may be predicted using Eq.(1):

$$F = \left(\delta_1\right)\left(\delta_2\right)\sigma_p A_{ps} \tag{1}$$

4.1.1 Modification factor δ_1

Modification factor δ_1 accounts for the reduction in bonded perimeter in specimens with reduced cover, with values given in Eq.(2):

$$\begin{aligned} c &\geq 1.5\phi & \delta_1 &= 1.0 \\ 0 \leq c &< 1.5\phi & \delta_1 &= 0.8 \\ -0.5\phi \leq c &< 0 & \delta_1 &= 0.5 \\ -0.5\phi &< c & \delta_1 &= 0.0 \end{aligned} \tag{2}$$

The value of δ_1 is taken as 1.0 when c≥1.5ø, based on the minimum cover distance required for full bond of 7-wire strand in BS EN 1992-1-1 [26] (see §2.2.3). As half the bar diameter is exposed for cover distances of -0.5ø, a value of δ_1 = 0.5 was chosen, and conservatively applied to the range of -0.5ø ≤ c < 0. In the range 0 ≤ c ≤ 1.5ø, the value of δ_1 was calibrated against the peak load test data and chosen as 0.80, ensuring that all predictions presented in Table 7 remain on the conservative side.

4.1.2 Modification factor δ_2

Confinement to strand can be provided by 1) transverse reinforcement, which dominates in specimens with zero or negative cover; and/or 2) concrete cover, which dominates in specimens with larger cover distances.

The value for δ_2 is proposed in Eq.(3):

$$\delta_2 = \max\left(\left\{\delta_3\right\},\left\{\delta_4\right\}\right) \not> 1 \quad (3)$$

Where δ_3 is the effect of confinement from transverse reinforcement and δ_4 is the effect of confinement from cover. It is assumed that one or other of these dominate the confinement behaviour and that the effects are not additive. It is therefore suggested that the maximum value of the two be taken.

4.1.2.1 Effect of transverse reinforcement (δ_3)

The degree of passive confinement provided by transverse reinforcement is calculated using the approach proposed in the fib Model Code [16], as given in Eq.(4):

$$\delta_3 = k_d\left(K_{tr} - \alpha_t / 50\right) \geq 0.0, K_{tr} \leq 0.05 \quad (4)$$

$$K_{tr} = n_t A_{st} / \left(n_b \phi s_t\right) \quad (5)$$

Where n_t is the number of legs of confining reinforcement crossing a potential splitting failure surface at a section; A_{st} is the cross sectional area of one leg of a confining bar; s_t is the longitudinal spacing of confining reinforcement; n_b is the number of anchored bars or pairs of lapped bars in the potential splitting failure surface; ø is the diameter of the anchored bar.

For the specimens presented in this paper: $k_d = 20$; $K_{tr} = 0.05$; $\alpha_t = 0.5$.

4.1.2.2 Effect of cover (δ_4)

In order to transmit bond forces, BS EN 1992-1-1 [26] requires members to have a cover to strand of at least 1.5ø. The confining effect of cover on strand is incorporated as shown in Figure 14, where a cover distance of 1.5ø provides full confinement by the cover, with a linear reduction between 1.5ø and -0.5ø. At cover distances less than -0.5ø, the concrete provides zero confinement to the strand.

The value of δ_4 is given by Eq.(6):

$$\begin{aligned} c \geq 1.5\phi \quad & \delta_4 = 1.0 \\ -0.5\phi \leq c < 1.5\phi \quad & \delta_4 = \frac{c}{4\phi} + \frac{5}{8} \\ c < -0.5\phi \quad & \delta_4 = 0.0 \end{aligned} \tag{6}$$

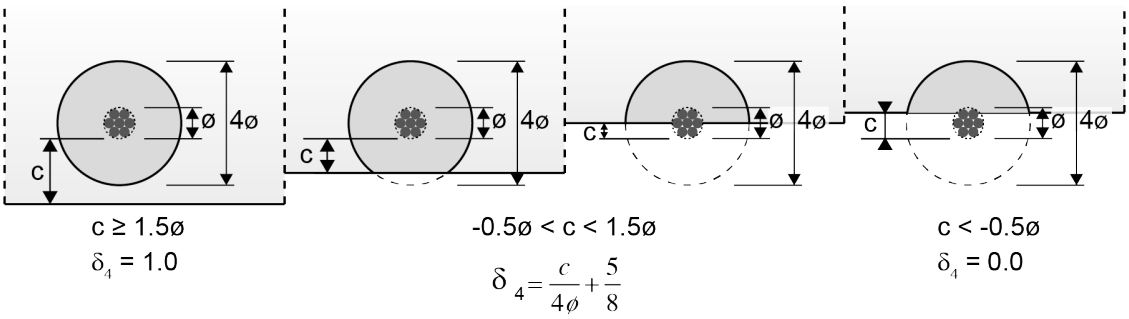

Figure 14: Definition of modification factor δ_4

4.1.3 Analysis

The effect of such an approach on BS EN 1992-1-1 [26] Figure 8.17 is illustrated in Figure 15, where l_{bpd} is the total anchorage length for anchoring a tendon with stress σ_{pd} as given by Eq.(7), l_{pt2} is 120% of the basic transmission length as given by Eq.(8), σ_{pd} is the tendon stress, σ_{pmoo} is the prestress after all losses, σ_{pm0} is the tendon stress just after release; α_1, α_2, η_{p1}, η_{p2}, and η_1 are parameters given in BS EN 1992-1-1 [26]; ϕ is the tendon diameter; f_{bpd} is the bond strength of the concrete at the test date as given by Eq.(9); f_{bpt} is the bond stress at transfer, given by Eq.(10); $f_{ctd(t)}$ is the axial tensile strength of the concrete at release; f_{ctd} is the axial tensile strength of the concrete.

$$l_{bpd} = l_{pt2} + \alpha_2 \phi \left(\sigma_{pd} - \sigma_{pm\infty} \right) / f_{bpd} \tag{7}$$

$$l_{pt2} = 1.2 \left(\alpha_1 \alpha_2 \phi \sigma_{pm0} / f_{bpt} \right) \tag{8}$$

$$f_{bpd} = \eta_{p2} \eta_1 f_{ctd} \tag{9}$$

$$f_{bpt} = \eta_{p1} \eta_1 f_{ctd(t)} \tag{10}$$

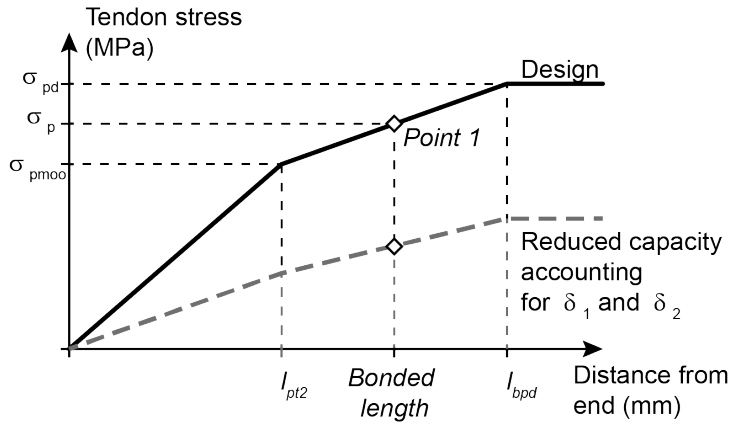

Figure 15: Stresses in the anchorage zone of pre-tensioned members

Once the values shown in Figure 15 are calculated, the tendon stress is predicted based on the available bonded length (600mm or 900mm in the tests described here). This point, shown as '*Point 1*' in Figure 15, provides a strand stress. Using Eq.(1) the predicted allowable anchorage force is then determined, multiplying the tendon stress from Figure 15 (σ_p calculated at available bonded length *l*) by the cross sectional area of the tendon and by the modification factors δ_1 and δ_2.

4.1.4 Peak capacity

The method described above was undertaken for all stressed specimens and is summarised in Table 7. Concrete properties are all values measured during testing from split cylinder tests: f_{ctd} in Eq.(9) is taken as $f_{ctm(te)}$, the mean axial tensile strength at the test date and $f_{ctd(t)}$ in Eq.(10) is taken as $f_{ctm(tr)}$, the mean axial tensile strength measured at transfer (concrete axial tensile strengths are obtained by multiplying split cylinder test results by 0.9).

As the prestress was monitored for all specimens from casting through to testing (Figure 7) the prestress after losses (σ_{pmoo}) is known accurately for all specimens.

Table 7: Peak capacity predictions for all stressed specimens

Code	δ_1	δ_2	δ_3	δ_4	$f_{ctm(tr)}$ (MPa)	l_{pt2} (mm)	$f_{ctm(te)}$ (MPa)	l_{bpd} (mm)	$\delta_1\delta_2(\sigma_{pd})$ (MPa)	$\delta_1\delta_2(\sigma_{pmoo})$ (MPa)	σ_p (MPa)	$F_{reduced}$ (kN)	Experimental (kN)	Exp/ Pred
55/E/600/37	1.00	1.00	0.80	1.00	2.25	440	3.50	1211	1670	551	783	109	217	1.99
55/E/600/0	0.80	0.80	0.80	0.63	3.59	276	3.38	1167	1069	268	559	78	105	1.35
55/E/600/-8	0.50	0.80	0.80	0.49	2.39	416	2.25	1744	668	171	240	33	84	2.52
69/E/900/37	1.00	1.00	0.80	1.00	2.14	580	2.02	1467	1670	926	1194	166	195	1.17
69/E/900/0	0.80	0.80	0.80	0.63	3.13	397	3.02	1216	1069	411	815	113	131	1.16
69/E/900/-8	0.50	0.80	0.80	0.49	3.64	341	3.67	981	668	277	618	86	129	1.50
55/U/600/37	1.00	1.00	0.00	1.00	3.47	286	2.96	935	1670	871	1257	175	233	1.33
55/U/600/0	0.80	0.63	0.00	0.63	2.30	431	2.61	1543	835	232	324	45	93	2.07
55/U/600/-8	0.50	0.49	0.00	0.49	3.73	266	3.82	1042	412	108	239	33	78	2.35
69/U/900/37	1.00	1.00	0.00	1.00	3.46	358	3.37	772	1670	1091	1670	232	264	1.14
69/U/900/0	0.80	0.63	0.00	0.63	3.82	325	3.37	1307	835	148	550	76	77	1.01
69/U/900/-8	0.50	0.49	0.00	0.49	3.37	368	3.22	1487	412	42	218	30	34	1.12
													Average	**1.56**
													COV	**34%**

It is seen that the proposed approach provides a generally conservative method for the prediction of peak capacity for specimens with reduced cover and a variety of internal reinforcement arrangements. The coefficient of variation is high, highlighting

that whilst conservative, the method should be applied with caution to specimens outside the boundaries of these data.

Specimen 69/U/900/-8 has unenclosed strand and -8mm cover. In this situation the strand has negligible confinement and any movement perpendicular to the applied load would cause the strand to 'peel off' from the concrete surface. Such perpendicular movement was indeed evident in this test, and came about as a direct result of the specimen rotating slightly, but significantly given the very low embedment depth. The 34kN load achieved in this specimen may be compared to 129kN achieved in 69/E/900/-8, where the test strand is enclosed by transverse reinforcement and, thus, peeling is prevented.

In most structures, prestress losses are not known accurately, and must be predicted by calculation. Taking a simplified approach of 25% typical losses and setting $\sigma_{pmoo} = 0.75(\sigma_{pm0})$ reduces the conservativeness of the peak capacity calculations, as shown in Table 8. Specimens 69/U/900/0 and 69/U/900/-8 now show unconservative predictions since actual losses were much higher than this simplified approach would suggest.

Table 8: Peak capacity predictions for all stressed specimens taking $\sigma_{pmoo} = 0.75(\sigma_{pm0})$

Code	δ_1	δ_2	δ_3	δ_4	$f_{ctm(tr)}$ (MPa)	l_{pt2} (mm)	$f_{ctm(te)}$ (MPa)	l_{bpd} (mm)	$\delta_1\delta_2(\sigma_{pi})$ (MPa)	$\delta_1\delta_2(\sigma_{pmoo})$ (MPa)	σ_p (MPa)	$F_{reduced}$ (kN)	Experimental (kN)	Exp/ Pred
55/E/600/37	1.00	1.00	0.80	1.00	2.25	440	3.50	1117	1670	687	919	128	217	1.70
55/E/600/0	0.80	0.80	0.80	0.63	3.59	276	3.38	976	1069	440	730	102	105	1.03
55/E/600/-8	0.50	0.80	0.80	0.49	2.39	416	2.25	1467	668	275	344	48	84	1.76
69/E/900/37	1.00	1.00	0.80	1.00	2.14	580	2.02	1547	1670	859	1127	157	195	1.24
69/E/900/0	0.80	0.80	0.80	0.63	3.13	397	3.02	1043	1069	550	954	133	131	0.99
69/E/900/-8	0.50	0.80	0.80	0.49	3.64	341	3.67	873	668	344	668	93	129	1.39
55/U/600/37	1.00	1.00	0.00	1.00	3.47	286	2.96	1085	1670	687	1073	149	233	1.56
55/U/600/0	0.80	0.63	0.00	0.63	2.30	431	2.61	1338	835	344	435	60	93	1.54
55/U/600/-8	0.50	0.49	0.00	0.49	3.73	266	3.82	885	412	169	300	42	78	1.87
69/U/900/37	1.00	1.00	0.00	1.00	3.46	358	3.37	938	1670	859	1617	225	264	1.17
69/U/900/0	0.80	0.63	0.00	0.63	3.82	325	3.37	905	835	429	832	116	77	0.67
69/U/900/-8	0.50	0.49	0.00	0.49	3.37	368	3.22	974	412	212	388	54	34	0.63
													Average	**1.30**
													COV	**32%**

It should be noted that the total prestress losses between tensioning and casting (Table 4) are particularly high for specimens 69/U/900/0 and 69/U/900/-8 (76% and

87% respectively). This degree of prestress loss implies that the strand had slipped significantly before testing, breaking the bond of the strand to concrete. This explains the unconservative predictions for these specimens, which are based on the assumption that some initial bond exists.

4.2 Bond-slip modelling

No broadly accepted model for the bond-slip behaviour of 7-wire strand is currently available. The fib Model Code [16] provides an analytical bond stress-slip relationship for deformed and plain bars that is based on Figure 16 and Eqs.(11)-(14). The bond stress-slip relationship is influenced by factors which include (i) surface geometry of the bar; (ii) concrete strength; (iii) casting position; (iv) cover distance; and (v) transverse confinement, either by reinforcement or applied load.

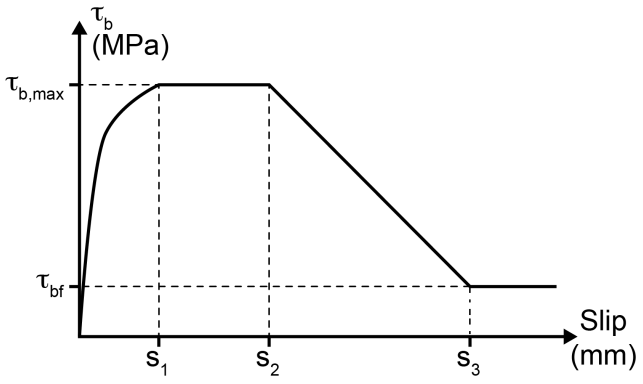

Figure 16: Bond stress-slip model basis [16]

$$\tau_{b0} = \tau_{b\max}\left(s / s_1\right)^{\alpha} \quad \text{for } 0 \le s \le s_1 \qquad (11)$$

$$\tau_{b0} = \tau_{b\max} \quad \text{for } s_1 < s \le s_2 \qquad (12)$$

$$\tau_{b0} = \tau_{b\max} - \left(\tau_{b\max} - \tau_{bf}\right)\left(s - s_2\right)/\left(s_3 - s_2\right) \quad \text{for } s_2 < s \le s_3 \qquad (13)$$

$$\tau_{b0} = \tau_{bf} \quad \text{for } s_3 < s \qquad (14)$$

The fib Model shown above predicts that deformed bar will achieve a greater peak bond stress (τ_{bmax}) when compared to plain bar, due primarily to the surface geometry of the bar which creates mechanical resistance to slip. In well-confined concrete a plateau at high bond stress can occur during crushing of the concrete between ribs. In unconfined concrete, a large drop in bond stress post-peak would instead be seen in a splitting failure mode.

For plain bar, once chemical bond is overcome the bar offers little further mechanical resistance to pull out. This is manifested in Figure 16 by setting $\tau_{b,max} = \tau_{bf}$ and $s_1 = s_2 = s_3$. The bond stress-slip behaviour of plain bar occurs at much lower stress levels when compared to deformed bar.

The test results demonstrate that the bond stress-slip behaviour of strand does not have the characteristic peak of deformed bar (where $\tau_{bmax} > \tau_{bf}$). This is shown for a sample of stressed specimens in Figure 17 and a sample of unstressed specimens in Figure 18. The test data provides only an average bond stress along the bar, as the load in the bar and the slip of the bar could only be measured in one place. This is a clear limitation that neglects the potential for variations in bond along the stressed length of a pull-out test.

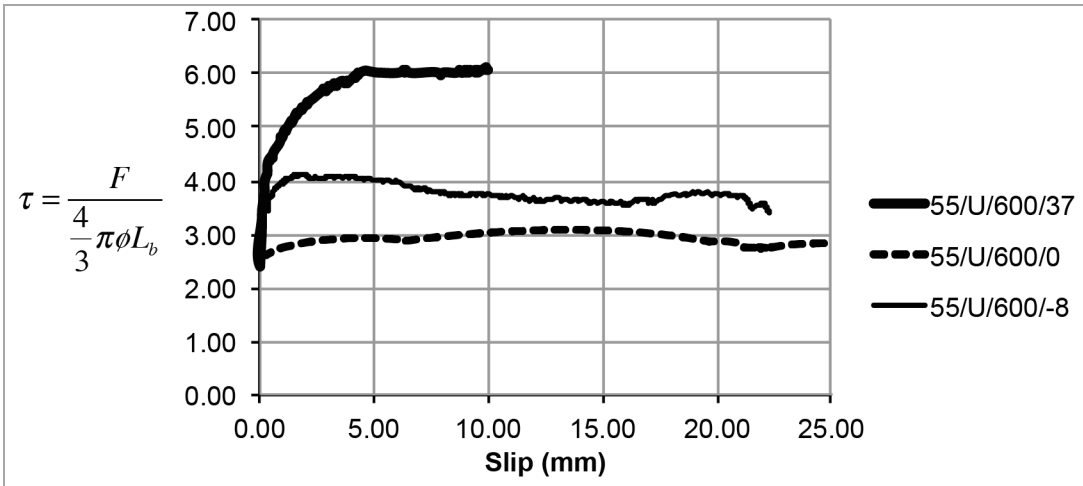

471

472 **Figure 17: Bond stress-slip (three stressed specimens)**

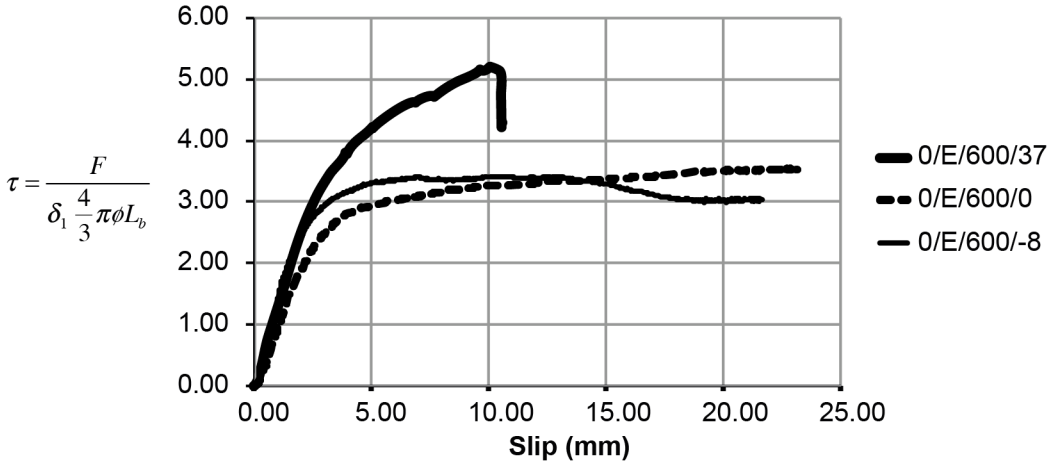

473

474 **Figure 18: Bond stress-slip (three unstressed specimens)**

475 Inspection of the specimens after testing showed that concrete was not crushed
476 between the strand wires (Figure 19). Therefore the plain bar model from the fib Model
477 Code [16] was adapted to produce a strand pull out model as described below.

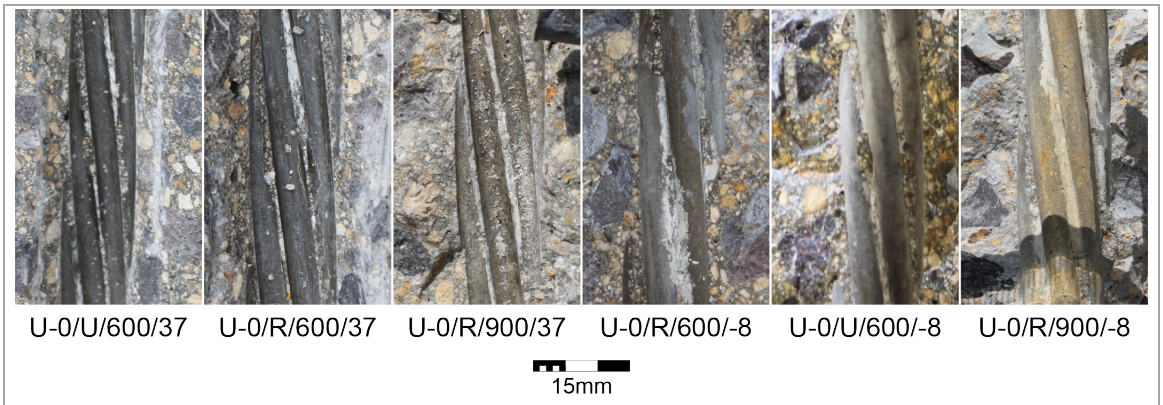

478

479 **Figure 19: Post-testing examination of concrete surface**

480 ### 4.2.1 Strand pull out model

481 The proposed bond stress model is based on the plain bar pull out model of the fib
482 Model Code [16] method and Eqs.(11)-(14). Proposed parameters for the model are
483 given in Table 9.

484 **Table 9: Proposed parameters for the strand pull out model**

Parameter	Proposed value – stressed 7-wire strand	Proposed value – unstressed 7-wire strand
$s_1 = s_2 = s_3$ (after FIB [16] and as shown in Figure 16)	0.1mm	2.0mm
α	0.5	0.5
$\tau_{b,max} = \tau_{bf}$	Eq.(15)	Eq.(15)

485 $$\tau_{b\max} = \tau_{bf} = (\delta_1)(\delta_2)(0.70)\sqrt{f_{cm}} \quad (15)$$

486 Where δ_1 accounts for the reduction in bonded perimeter in specimens with reduced
487 cover (Eq.(2); δ_2 accounts for confinement from cover or transverse reinforcement
488 (Eq.(3)); the factor of 0.70 is chosen based on the test results; f_{cm} is the mean concrete
489 cylinder strength of the specimen.

490 The experimental bond stress is compared to the proposed model in Table 10 for
491 stressed strand specimens and in Table 11 for the unstressed strand specimens. The
492 bond stress is calculated using Eq.(16), following the method used by both Mattock (as

cited by Tabatabai and Dickson [39]) and Marti-Vargas *et al* [40] to calculate the actual circumference from nominal strand diameter:

$$\tau = \frac{F}{\delta_1 \frac{4}{3}\pi\phi L_b} \quad (16)$$

where F is the force in the strand; ø is the nominal strand diameter; δ_1 accounts for reduction in bonded perimeter with reduced cover; and L_b is the bonded length. The peak bond stress during testing is found by setting $F = F_{max}$, the maximum recorded force in the strand during testing.

Table 10: Predicted peak bond stress for stressed strand specimens using Eq.(15)

Code	f_{cm} (MPa)[a]	δ_1	δ_2	δ_3	δ_4	Cover (mm)	Bonded length (mm)	Failure load (kN)	Experimental peak stress (MPa)	Predicted peak stress[b] (MPa)	Experimental / Predicted
55/E/600/37	42.2	1.00	1.00	0.80	1.00	37	600	217	5.68	4.55	1.25
55/E/600/0	42.9	0.80	0.80	0.80	0.63	0	600	105	3.44	2.93	1.17
55/E/600/-8	46.6	0.50	0.80	0.80	0.49	-8	600	84	4.40	1.91	2.30
69/E/900/37	43.8	1.00	1.00	0.80	1.00	37	900	232	4.05	4.63	0.87
69/E/900/0	36.3	0.80	0.80	0.80	0.63	0	900	131	2.86	2.70	1.06
69/E/900/-8	46.8	0.50	0.80	0.80	0.49	-8	900	129	4.50	1.92	2.35
55/U/600/37	43.4	1.00	1.00	0.00	1.00	37	600	233	6.10	4.61	1.32
55/U/600/0	43.7	0.80	0.63	0.00	0.63	0	600	93	3.04	2.31	1.32
55/U/600/-8	47.8	0.50	0.49	0.00	0.49	-8	600	78	4.08	1.19	3.42
69/U/900/37	39.0	1.00	1.00	0.00	1.00	37	900	264	4.61	4.37	1.05
69/U/900/0	47.0	0.80	0.63	0.00	0.63	0	900	77	1.68	2.40	0.70
69/U/900/-8	46.2	0.50	0.49	0.00	0.49	-8	900	34	1.19	1.17	1.01
										Average	**1.49**
										COV	**53%**

Notes: [a] mean concrete cylinder strength of the specimen; [b] Eq.(14)

The results are illustrated for Specimens 55/U/600/37, 55/U/600/0, and 55/U/600/-8 in Figure 20. The predictions are on average conservative, but the coefficient of variation is high. Specimens 69/E/900/37 and 69/U/900/0 have mildly unconservative peak bond stress predictions (average 0.79). The high variation is in part due to the changing surface area for which the experimental peak stress is calculated. In addition Eq.(15) does not account for effects in the bonded length of the specimen. In specimens with 0mm or -8mm cover the strand may be fully debonded over a portion

of the intended bond length, meaning that the true bond stress in the bonded portion would be higher than is predicted by Eq.(15).

$$\tau = \frac{F}{\delta_1 \frac{4}{3}\pi\phi L_b}$$

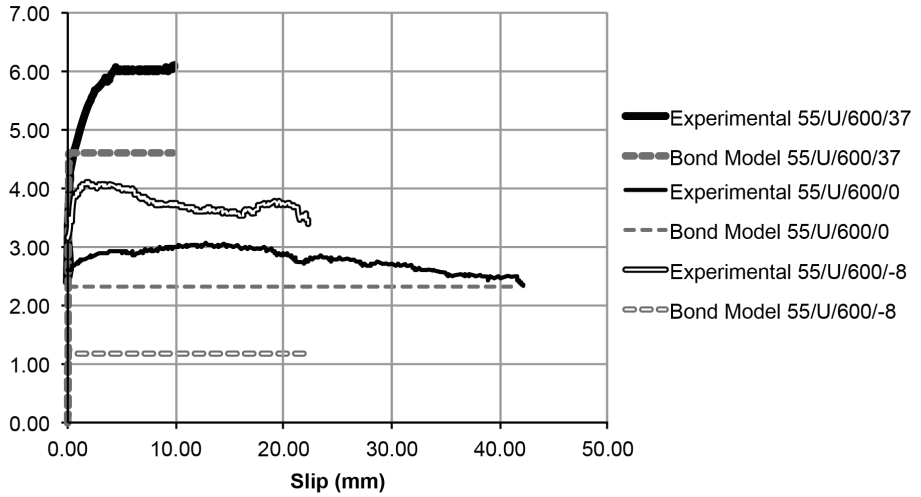

Figure 20: Comparison of experimental and bond model results for specimens 55/U/600/37, 55/U/600/0, and 55/U/600/-8

Table 11: Predicted bond stress for unstressed strand specimens using Eq.(15)

Code	f_{cm} (MPa)[a]	δ_1	δ_2	δ_3	δ_4	Cover (mm)	Bonded length (mm)	Failure load (kN)	Experimental peak stress (MPa)	Predicted peak stress[b] (MPa)	Experimental / Predicted
0/P/300/37	42.7	1.00	1.00	0.00	1.00	37	300	85	4.45	4.58	0.97
0/P/300/0	42.7	0.80	0.63	0.00	0.63	0	300	50	3.27	2.29	1.43
0/P/600/37	46.6	1.00	1.00	0.00	1.00	37	600	208	5.44	4.78	1.14
0/P/600/0	46.0	0.80	0.63	0.00	0.63	0	600	79	2.58	2.37	1.09
0/E/300/37	39.8	1.00	1.00	0.80	1.00	37	300	111	5.81	4.42	1.32
0/E/300/0	39.8	0.80	0.80	0.80	0.63	0	300	65	4.25	2.83	1.50
0/E/300/-8	39.3	0.50	0.80	0.80	0.49	-8	300	52	5.44	1.75	3.10
0/E/600/37	42.7	1.00	1.00	0.80	1.00	37	600	199	5.21	4.57	1.14
0/E/600/0	45.8	0.80	0.80	0.80	0.63	0	600	108	3.53	3.03	1.17
0/E/600/-8	43.3	0.50	0.80	0.80	0.49	-8	600	65	3.40	1.84	1.85
0/E/900/37	41.6	1.00	1.00	0.80	1.00	37	900	223	3.89	4.51	0.86
0/E/900/0	42.3	0.80	0.80	0.80	0.63	0	900	159	3.47	2.91	1.19
0/E/900/-8	34.7	0.50	0.80	0.80	0.49	-8	900	124	4.33	1.65	2.62
0/U/600/37	41.7	1.00	1.00	0.00	1.00	37	600	216	5.65	4.52	1.25
0/U/600/0	40.6	0.80	0.63	0.00	0.63	0	600	83	2.72	2.23	1.22
0/U/600/-8	46.3	0.50	0.49	0.00	0.49	-8	600	77	4.03	1.18	3.43
0/U/900/37	48.1	1.00	1.00	0.00	1.00	37	900	250	4.36	4.86	0.90
0/U/900/0	47.3	0.80	0.63	0.00	0.63	0	900	136	2.97	2.41	1.23
0/U/900/-8	46.2	0.50	0.49	0.00	0.49	-8	900	112	3.91	1.17	3.33
										Average	1.62
										COV	52%

Notes: [a] mean concrete cylinder strength of the specimen; [b] Eq.(14)

The results are illustrated for Specimens 0/E/600/37, 0/E/600/0, and 0/E/600/-8 in Figure 21. The predictions shown in Table 11 are on average conservative, but the

coefficient of variation is again high. Specimens 0/P/300/37, 0/E/900/37 and 0/U/900/37 have mildly unconservative peak bond stress predictions (average 0.91).

The high variability in both data sets could be attributable to the specimens with partially exposed strand. If specimens with -8mm cover are excluded from the analysis, the stress predictions are improved slightly. For stressed specimens, the average ratio is 1.09 with a COV of 20%; for unstressed specimens the ratio is 1.17 with a COV of 16%.

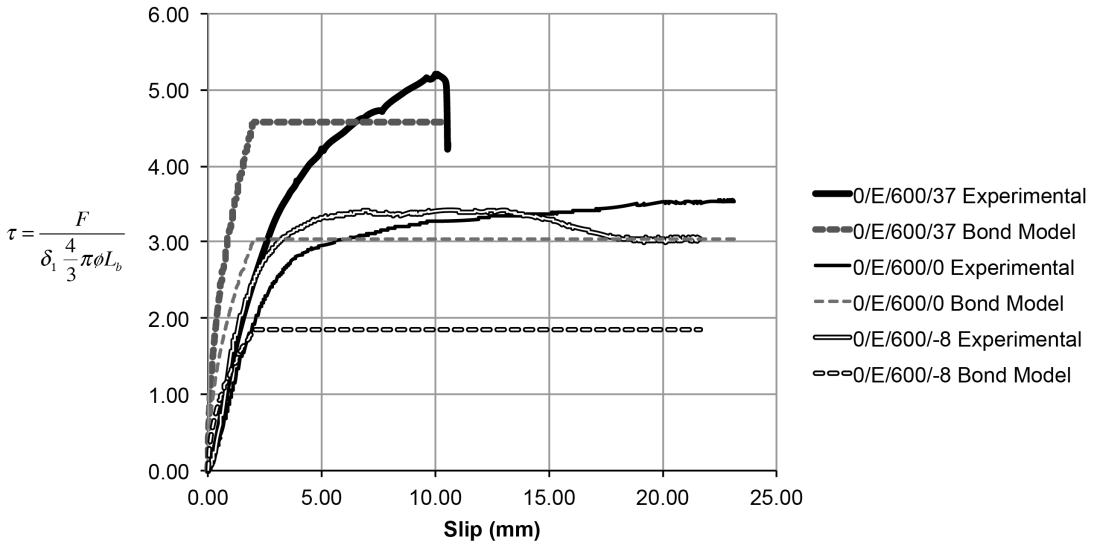

Figure 21: Comparison of experimental and bond model results for specimens 0/E/600/37, 0/E/600/0, and 0/E/600/-8

5 Discussion

Accurately determining the behaviour of concrete elements suffering from loss of cover is of crucial importance when high cost infrastructure is being assessed. A full understanding of capacity can allow load restrictions and closures to be minimised prior to appropriate repair work.

In this paper it is seen that as cover distances are reduced, ultimate (peak) capacities and residual capacities also reduce. Specimens with unstressed strand lost

up to 67% capacity at -8mm cover when compared to 37mm cover, while specimens with stressed strand lost up to 87% capacity at -8mm cover when compared to 37mm cover.

Detailing practice of reinforced concrete members has changed considerably over time, and varies between countries. It is seen that specimens with unenclosed strand, where the transverse reinforcement does not enclose the longitudinal reinforcement, achieved surprisingly high peak capacities. 0/U/600/-8 (unstressed, unenclosed strand with -8mm cover) reached 35% of the capacity of 0/U/600/37 (unstressed, unenclosed strand with 37mm cover).

However, it was generally seen that specimens with -8mm and 0mm cover whose strand was enclosed by transverse reinforcement reached a higher peak load than those whose strand was unenclosed, due to the additional confining effect of the transverse reinforcement. In only one case did an unenclosed specimen, 0/U/600/-8, achieved a higher load than the equivalent enclosed specimen, 0/E/600/-8. Specimens with unenclosed strand typically demonstrated post-peak behaviour with a descending load-slip curve.

Specimens with less than 0mm cover (i.e. with partially exposed strand) demonstrate highly variable results when attempts are made to predict bond stresses. Small variations in the cover distance, caused by normal construction tolerances, may be critical for this set of tests. A small change in cover distance would potentially lead to a significant percentage change in bonded area and pull out capacity. As shown in §4.2.1, the coefficient of variation of the capacity predictions is improved by excluding negative cover specimens from the analysis. Since only one specimen was tested for each combination of transverse reinforcement arrangement, bond length and cover distance, an accurate measure of this degree of variability is not known.

In addition to the pull out testing, the monitoring of strand stress through the casting and detensioning process has provided useful data. Stressed beams with full cover (37mm) saw lower losses between tensioning and testing than those with 0mm and -8mm cover. Specimens 55/U/600/37 and 69/U/900/37, with 37mm cover, both lost 13% of their prestress between tensioning and testing. This compares to losses of up to 76% for 69/U/900/0 (0mm cover) and 87% for 69/U/900/-8 (-8mm cover). In both of these situations, the degree of prestress loss has significantly influenced subsequent pull out testing, as the strand can be assumed to have lost significant bond during detensioning prior to testing.

The method provides good predictions of peak bond capacity for both stressed and unstressed strand that provides conservative results for all specimens (Table 7).

The behaviour of strand during pull out is seen to be similar to plain bar, with a characteristic plateau, but achieves higher bond stresses than would be predicted by a plain bar pull out model. A strand bond stress-slip relationship is proposed, based on the general model given in the fib Model Code [16]. The relationship proposed in Eq.(15) is, on average, conservative for both stressed and unstressed specimen. However, considerable variability in the predictions is again seen (Table 10 and Table 11) suggesting that further work is required to identify the controlling parameters for bond modelling.

The test results show good correlation between the stressed and unstressed tests undertaken in this investigation, demonstrating that the unstressed method is a suitable proxy for the stressed behaviour. This paper has considered the behaviour of specimens with reduced cover, but does not consider other effects such as corrosion to strands, which may also occur in field conditions.

5.1 Conclusions

The periodic assessment of our existing infrastructure is a crucial part of maintaining appropriate levels of public safety over long periods of time. It is important that realistic predictions of the capacity of existing structures can be made in order to avoid unnecessary and expensive intervention work.

This paper has addressed this issue for the case of prestressed concrete beams, which face two main assessment challenges – 1) design and construction practice has changed significantly in the past 50 years, and modern codified approaches can be incompatible with historic designs; and 2) deterioration of exposed soffits can lead to reduced cover to internal prestressing strand.

There are currently no widely accepted methods for the prediction of the peak and residual capacity of prestressed concrete beams with inadequately detailed 7-wire strand. This paper presents a new predictive model that has been validated against a new set of experimental results from 31 beam tests, including 19 with unstressed strand and 12 with stressed strand.

This paper has investigated in detail for the first time the effect of loss of cover on bond, peak load, and residual load in structures where 7-wire strand is used as flexural reinforcement. The results presented here may be used to support new guidance on appropriate reduction factors for assessment of prestressed concrete elements with inadequately detailed 7-wire strand.

5.2 Future work

In addition to the developments made in this paper, further work is required to fully understand the behaviour of structures deemed to be structurally inadequate. The impact of the in-situ corrosion of strand on bond performance and the effectiveness of

609 repairs to structures with reduced or ineffective cover, are both areas of great
610 importance that need further work.

611 ## 5.3 Acknowledgements

612 This work was commissioned by Balfour Beatty Mott MacDonald JV, the Asset Support
613 Contract Provider for Highways England Area 10, as part of a Research project to
614 investigate the actual capacity of half-joints with theoretically inadequate reinforcement
615 detailing. The authors gratefully acknowledge support and advice from Highways
616 England in the preparation of the test program and this paper, and the technician
617 support provided by the University of Bath in constructing and testing the specimens.

618

619

References

[1] ASCE. Infrastructure Report Card. ASCE; 2016.

[2] HM Treasury. National Infrastructure Plan 2014. London: HM Treasury; 2014.

[3] Highways Agency. BD57. DESIGN FOR DURABILITY. London: The Stationery Office; 2001.

[4] Highways Agency. BD 44/15. The Assessment of Concrete Highway Bridges and Structures. London: The Stationery Office; 2015.

[5] Highways Agency. BA 39/93. ASSESSMENT OF REINFORCED CONCRETE HALF-JOINTS. London: The Stationery Office; 1993.

[6] The Highways Agency. BD 79/13. THE MANAGEMENT OF SUB-STANDARD HIGHWAY STRUCTURES. London: The Stationery Office; 2013.

[7] RILEM. RILEM Recommendations for the Testing and Use of Constructions Materials, RC 5 Bond test for reinforcement steel. 1. Beam test. London: E & FN SPON; 1982.

[8] ASTM. D7913-14. Standard Test Method for Bond Strength of Fiber-Reinforced Polymer Matrix Composite Bars to Concrete by Pullout Testing. West Conshohocken, PA: ASTM International; 2014.

[9] Haskett M, Oehlers DJ, Ali MS. Local and global bond characteristics of steel reinforcing bars. Engineering Structures. 2008;30:376-83.

[10] Metelli G, Plizzari G. influence of the relative rib area on bond behaviour. Magazine of Concrete Research. 2014;66:277-94.

[11] Cairns J, Plizzari G. Towards a harmonised European bond test. Materials and Structures. 2003;36:498-506.

[12] fib. Bond of reinforcement in concrete. State of art report task group Bond Models. Lausanne: fib; 2000.

[13] BSI. BS 4449:2005+A3:2016. Steel for the reinforcement of concrete Weldable reinforcing steel Bar, coil and decoiled product Specification. London: BSI; 2016.

[14] ASTM. A944 - 10. Standard Test Method for Comparing Bond Strength of Steel Reinforcing Bars to Concrete Using Beam-End Specimens. West Conshohocken, PA: ASTM International; 2015.

[15] Perera K, Ibell T, Darby A. Bond characteristics of near surface mounted CFRP bars. Construction and Building Materials. 2013;43:58-68.

655 [16] FIB. Model Code 2010. Volume 1. Lausanne: International
656 Federation of Structural Concrete (fib); 2013.
657 [17] Moustafa S. Pull-out strength of strand and lifting loops. Washington:
658 Concrete Technology Corporation; 1974.
659 [18] Ramirez JA, Russell BW. Transfer, Development, and Splice Length
660 for Strand/Reinforcement in High-Strength Concrete. NCHRP REPORT
661 603 ed. Washington, DC: Transportation Research Board; 2008.
662 [19] ASTM. A1081. Standard Test Method for Evaluating Bond of Seven-
663 Wire Steel Prestressing Strand. West Conshohocken: ASTM International;
664 2012.
665 [20] Logan DR. Acceptance Criteria for Bond Quality of Strand for
666 Pretensioned Prestressed Concrete Applications. PCI Journal. 1997;March-
667 April:52-90.
668 [21] Rose DR, Russell BW. Investigation of Standardized Tests to Measure
669 the Bond Performance of Prestressing Strand. PCI Journal. 1997;July-
670 August:56-80.
671 [22] Briere V, Harries K, Kasan J, Hager C. Dilation behavior of seven-
672 wire prestressing strand – the Hoyer effect. Constr Build Mater.
673 2013;40:650-8.
674 [23] Marti-Vargas JR, Serna-Ros P, Fernandez-Prada MA, Miguel-Sosa
675 PF. Test method for determination of the transmission and anchorage
676 lengths in prestressed reinforcement. Magazine of Concrete Research.
677 2006;58:21-9.
678 [24] Cousins TE, Badeaux MH, Moustafa S. Proposed test for determining
679 bond characteristics of prestressing strand. PCI Journal. 1992;January-
680 February:66-73.
681 [25] Barnes RW, Burns NH. Anchorage Behavior of 15.2 mm (0.6 in)
682 Prestressing Strand in High Strength Concrete. PCI/FHWA/FIB
683 International Symposium on High Performance Concrete. Orlando, FL:
684 PCI; 2000. p. 484–93.
685 [26] BSI. BS EN 1992-1-1. Eurocode 2: Design of concrete structures -
686 Part 1-1: General rules and rules for buildings. London, UK: BSI; 2004.
687 [27] Tepfers R. A Theory of Bond Applied to Overlapping Tensile
688 Reinforcement Splices for Deformed Bars. Division of Concrete
689 Structures: Chalmers University of Technology, Goteborg, Sweden; 1973.
690 p. 328.

691 [28] Galvez JC, Benitez JM, Tork B, Casati MJ, Cendon DA. Splitting
692 failure of precast prestressed concrete during the release of the prestressing
693 force. Engineering Failure Analysis. 2009;16:2618-34.
694 [29] Den Uijl JA, Bigaj AJ. A bond model for ribbed bars based on
695 concrete confinement. HERON. 1996;41:201-26.
696 [30] Deatherage JH, Burdette EG. Development length and lateral spacing
697 requirements of prestressing strand for prestressed concrete bridge girders.
698 PCI Journal. 1994;January-February:70-83.
699 [31] Den Uijl JA. Transfer length of prestressing strand in HPC. Progress
700 in Concrete Research. 1995;4:75-90.
701 [32] Rogers RA, Wotherspoon L, Scott A, Ingham J. Residual strength
702 assessment and destructive testing of decommissioned concrete bridge
703 beams with corroded pretensioned reinforcement. PCI Journal.
704 2012;Summer 2012.
705 [33] BSI. BS 12390-2. Testing hardened concrete Part 2: Making and
706 curing specimens for strength tests. London: BSI; 2009.
707 [34] BSI. BS EN 12390-3. Testing hardened concrete Part 3: Compressive
708 strength of test specimens. London, UK: BSI; 2009.
709 [35] BSI. BS EN 12390-6. Testing hardened concrete Part 6: Tensile
710 splitting strength of test specimens. London, UK: BSI; 2009.
711 [36] BSI. BS 4449. Steel for the reinforcement of concrete Weldable
712 reinforcing steel Bar, coil and decoiled product Specification. London:
713 BSI; 2005.
714 [37] Bridon. High quality prestressing wire & strand for construction
715 product applications. Construction Products. Doncaster: Bridon; ND.
716 [38] BSI. prEN 10138-3. Prestressing steels - Part 3: Strand. London: BSI;
717 2000.
718 [39] Tabatabai H, Dickson TJ. The History of the Prestressing Strand
719 Development Length Equation. PCI Journal. 1993;38.
720 [40] Marti-Vargas JR, Serna P, Hale WM. Strand bond performance in
721 prestressed concrete accounting for bond slip. Engineering Structures.
722 2013;51:236-44.
723